MABS
2018, VOL. 10, NO. 7, 1073–1083
https://doi.org/10.1080/19420862.2018.1504726

Taylor & Francis
Taylor & Francis Group

REPORT

High-throughput screening of antibody variants for chemical stability: identification of deamidation-resistant mutants

Danielle M. DiCara[a], Nisana Andersen[b], Ruby Chan[c]*, James A. Ernst[c,d], Gai Ayalon[d]†, Greg A. Lazar[a], Nicholas J. Agard[a], Amy Hilderbrand[c]‡, and Isidro Hötzel[a]

[a]Department of Antibody Engineering, Genentech Inc., South San Francisco, CA, USA; [b]Protein Analytical Chemistry, Genentech Inc., South San Francisco, CA, USA; [c]Department of Protein Chemistry, Genentech Inc., South San Francisco, CA, USA; [d]Department of Neuroscience, Genentech Inc., South San Francisco, CA, USA

ABSTRACT

Developability assessment of therapeutic antibody candidates assists drug discovery by enabling early identification of undesirable instabilities. Rapid chemical stability screening of antibody variants can accelerate the identification of potential solutions. We describe here the development of a high-throughput assay to characterize asparagine deamidation. We applied the assay to identify a mutation that unexpectedly stabilizes a critical asparagine. Ninety antibody variants were incubated under thermal stress in order to induce deamidation and screened for both affinity and total binding capacity. Surprisingly, a mutation five residues downstream from the unstable asparagine greatly reduced deamidation. Detailed assessment by LC-MS analysis confirmed the predicted improvement. This work describes both a high-throughput method for antibody stability screening during the early stages of antibody discovery and highlights the value of broad searches of antibody sequence space.

ARTICLE HISTORY
Received 14 February 2018
Revised 4 July 2018
Accepted 18 July 2018

KEYWORDS
Antibodies; developability; HTP developability assessment; asparagine deamidation; surface plasmon resonance; therapeutic antibody development

Introduction

Biological therapeutics, including antibodies, are susceptible to chemical and physical modifications that can alter their drug-like properties.[1,2] Currently, production processes for biologics are designed to remove degradation products,[1,2] and the biologics are formulated to increase stability.[1,3-6] Identification of antibodies that are stable throughout expression, purification, formulation, storage, distribution and in vivo is expected to reduce development and production costs, increase product shelf-life and improve potency in vivo if the chemical liability affects target binding or antibody pharmacokinectics.[1-6] Thus, it is increasingly common to include pharmaceutical developability as a criterion in the selection of development candidates.[7-9] Early identification of potential liabilities may enable selection of candidates with more suitable properties or the mitigation of specific liabilities through engineering, prior to resource-intensive manufacturing and formulation activities.[8] While multiple modifications can alter an antibody's chemical structure during production, in this work we focus on screening for antibody variants that resolve chemical deamidation of asparagine residues.

Spontaneous deamidation of asparagine residues is a common and irreversible protein modification in which the asparagine side-chain amide is converted to a carboxylic acid. Deamidation of solvent-exposed asparagine residues on proteins proceeds via formation of a short-lived succinimide intermediate and yields up to four different products, specifically aspartic acid (Asp) and iso-aspartic acid (iso-Asp) as both L and, less prevalently, D stereoisomers[10,11], (Figure 1). The reaction affects protein charge and structure because all four products contain an additional negative charge compared to the parental asparagine, and, in the case of iso-Asp formation,[11] the polypeptide backbone is altered as well as the side chain.

Deamidation does not necessarily affect all asparagine residues in a polypeptide equally. Factors known to influence the rate of asparagine deamidation include the primary sequence,[13,14] particularly the nature of the amino acid in the +1 position;[15] pH;[16] temperature;[10,11] buffer ions;[16] and the three-dimensional (3D) structure.[17] Given the importance of the 3D structural environment, methods that calculate the deamidation rate for specific asparagine residues require access to a high resolution structural model.[18-20] In the absence of high resolution structural data or an accurate molecular model, understanding deamidation tendencies within proteins requires empirical analysis.

The current "gold standard" for post-translational modification analysis of biotherapeutics involves enzymatic digestion of the protein into peptides that are then analyzed by liquid chromatography (LC) coupled to tandem mass spectrometry (MS).[21] However, care must be taken to avoid introduction of

CONTACT Danielle M. DiCara dicara.danielle@gene.com; Isidro Hötzel hotzel.isidro@gene.com Department of Antibody Engineering, Genentech Inc., 1 DNA Way, South San Francisco, CA 94080, USA

*Current address: Gilead Sciences, Foster City, CA, 94404, USA.
†Current address: Alector, 151 Oyster Point Blvd, Suite 300, South San Francisco CA 94080.
‡Current address: Fitbit, 405 Howard Street, Suite 550, San Francisco, CA, 94105, USA.

Color versions of one or more of the figures in the article can be found online at www.tandfonline.com/kmab.
Supplementary materials can be accessed here

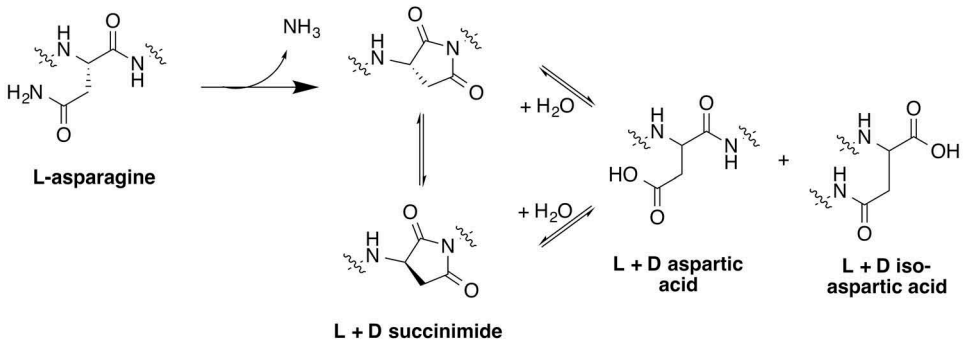

Figure 1. Asparagine side chain deamidation products and intermediates.

Cyclization of asparagine to succinimide involves the loss of the amine group and is considered irreversible under physiological conditions.[3] Hydrolysis of succinimide results in reversible generation of aspartic acid and iso-aspartic acid. Asparagine deamidation can also result in generation of the epimers D-Asp and D-iso-Asp.[11] The ratio of iso-Asp to Asp generated by asparagine deamidation in the context of an Asn-Gly (NG) motif under approximately physiological conditions is about 3:1.[12]

artifacts during sample processing,[22-24] and, although high-throughput (HTP) approaches have been reported,[24] these methods are not currently routine and require substantial automation, as well as MS instrumentation and expertise. Alternative HTP methods for deamidation detection are typically indirect, for example, reverse-phase HPLC to detect changes in polarity and hydrophobicity, and ion exchange chromatography or electrophoresis based methods to detect changes in charge.[25,26] The enzyme protein L-isoaspartyl methyltransferase (PIMT), which catalyzes methylation of L-iso-Asp,[27,28] has been utilized to develop high-throughput biochemical assays for iso-Asp quantitation;[29] however, detection of iso-Asp is not necessarily an indicator of deamidation and PIMT-based methods have the potential to produce false negative results in cases where formation of iso-Asp is hindered.[30,31] A need still exists therefore for low-cost, sensitive, quantitative methods for HTP screening of antibody candidates for chemical modifications.

Target binding assays present an attractive and complementary approach to biophysical methods for the detection and monitoring of post-translational modifications, since changes in binding can potentially reflect issues arising from primary, secondary, tertiary or quaternary structure, as well as cumulative negative impacts arising from multiple slightly deleterious mutations. Assays that use binding to target protein as a surrogate measure for antibody activity,[8,32-36] are particularly useful for developability assessment at the antibody discovery and engineering stage, as they focus specifically on changes that can potentially impact potency, regardless of the location or the type of modification. In combination with LC-MS peptide mapping, target binding assays can locate specific residues for targeting with focused engineering efforts. In addition, binding assays typically require extremely little protein and can be performed very rapidly.

Here, we describe a binding assay, which is based on an antibody capture surface plasmon resonance (SPR) assay that does not require a calibration curve to provide useful results, that can be used as an HTP screen to identify candidates for more rigorous, lower throughput site-specific deamidation analyses. We describe the use of this assay, coupled with microplate-format thermal stress tests, to identify a mutation that was confirmed using MS to unexpectedly stabilize a deamidation-prone asparagine located in the complementarity-determining region (CDR)-L1. The assay requires very little protein, is relatively simple to perform, and could in principle be applied to *de novo* antibody candidate screening and selection in addition to antibody engineering.

Results

Comparison of Antibody #1 SPR profile before and after stress demonstrates differential effects on the kinetics versus the magnitude of binding signal

During characterization of a humanized antibody (referred to here as antibody #1), we identified a potentially significant asparagine deamidation site located at residue position 28 (Kabat numbering) of the light chain variable region (VL). To evaluate the impact of this modification on target binding, we sought to generate a well-characterized mixture of purified antibody containing a significant percentage of deamidated antibody. Purified antibody #1 was subjected to stress conditions that promote deamidation: incubation at 37°C at pH 7.4 for 2 weeks. This resulted in an increase in nominal deamidation levels at VL.N28 from 22.6% ("control" sample) to 65.7% ("stressed" sample) (Table 1, Figure 2).

To understand the impact of the deamidation on binding, the control and stressed antibody samples were analyzed by SPR, using an antibody capture format (Figure 2). Equilibrium dissociation constants (KD) for the control and stressed samples were virtually indistinguishable (Table 1, Supplementary Figure 1). In contrast, the magnitude of the antigen-binding signal was noticeably reduced for the stressed sample in comparison to the control sample (Figure 2). The magnitude of analyte binding can be evaluated using the parameter Rmax, which here represents the projected maximum binding response when the captured antibody is saturated with antigen and the binding signal thus reaches a plateau. Since the size of this response will depend on the number of binding sites available, Rmax is dependent on the amount of antibody captured, termed the capture level.[37] We therefore normalized the Rmax values by dividing them by the

Table 1. N28 deamidation levels and SPR analysis of control and stressed Antibody #1 samples.

	Peptide Mapping			SPR Analysis				
	Nominal deamidated N28	Nominal intact N28	ΔNominal intact N28	Ligand Level (RU[a])	Rmax (RU[a])	KD[b] (nM)	nRmax	ΔnRmax
Control	22.6%	77.4%	56%	102.9	47.7	0.7	0.46	56%
Stressed	65.7%	34.3%		146.8	30.2	0.7	0.21	

[a]Resonance Units.
[b]Equilibrium dissociation constant.

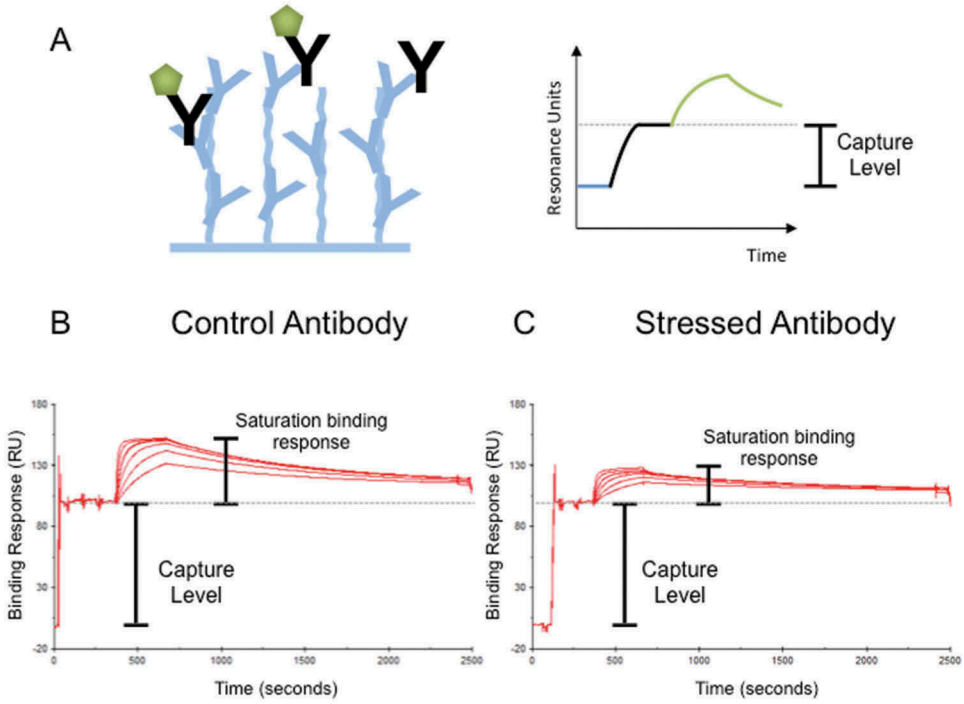

Figure 2. Control and stressed antibodies binding to soluble antigen in an antibody capture format SPR experiment.

A: Schematic illustrating the outline of the antibody capture SPR assay format used. The surface (pale blue) is prepared by covalent immobilization of an antibody binding protein,[37] which enables subsequent non-covalent capture of the test antibodies (black). The response due to antibody capture is termed the capture level.[37] After antibody capture, the surface is exposed to antigen (green shape & green curve) at a known concentration, and antigen binding at this concentration is monitored for a fixed period of time. The antigen solution is then replaced with buffer and antigen dissociation monitored for a fixed period of time. Finally, the surface is washed with a regeneration solution that dissociates the antibody (including any associated antigen) from the surface, and the cycle is repeated.B, C: SPR sensorgrams showing control (B) and stressed (C) samples of Antibody #1 binding to a human IgG capture chip, followed by binding of target antigen. Sensorgrams from multiple cycles are shown aligned and to assist comparison have been normalized to the antibody capture signal (capture level). Antibody capture signals prior to normalization are shown in Table 1.

relevant capture level. The normalized Rmax (nRmax) observed for the stressed sample was 56% lower than that of the control sample, matching the decrease of intact, non-deamidated N28 relative to the non-stressed sample as determined by MS (Table 1). The results are consistent with a reduction in the proportion of antigen binding sites per unit of antibody that remains competent to bind to the target antigen at a level that is detected under these conditions.

Mixing parental antibody and a surrogate deamidation product results in a similar SPR profile to that observed with the stressed parental antibody

In order to validate the correlation between N28 deamidation and reduction of antigen binding, we generated an N28D mutant of antibody #1. N28D mutation replicates one of the major deamidation products, and results in ~ 100-fold loss of affinity (Figure 3, Table 2). While it is not possible to produce alternative regio- and stereo-isomers of Asp using traditional recombinant DNA technology, the tight correlation between deamidation and loss of binding suggests that these species, if present, do not bind appreciably under these conditions. To mimic the contents of a partially-deamidated antibody sample, we prepared a mixture of parental and N28D antibody, and collected binding data using both the mixture and the individual antibodies. The results were first analyzed using a 1:1 binding model in order to obtain values for the ka and kd of the individual antibodies (Table 2). The data were then re-analyzed using a heterogenous ligand binding model in which, to reduce the number of variable parameters, one of the two interactions within the model was defined using the Antibody #1 ka and kd obtained with the 1:1 binding model (Table 2). For the mixture of Antibody #1 with the N28D mutant, the modified

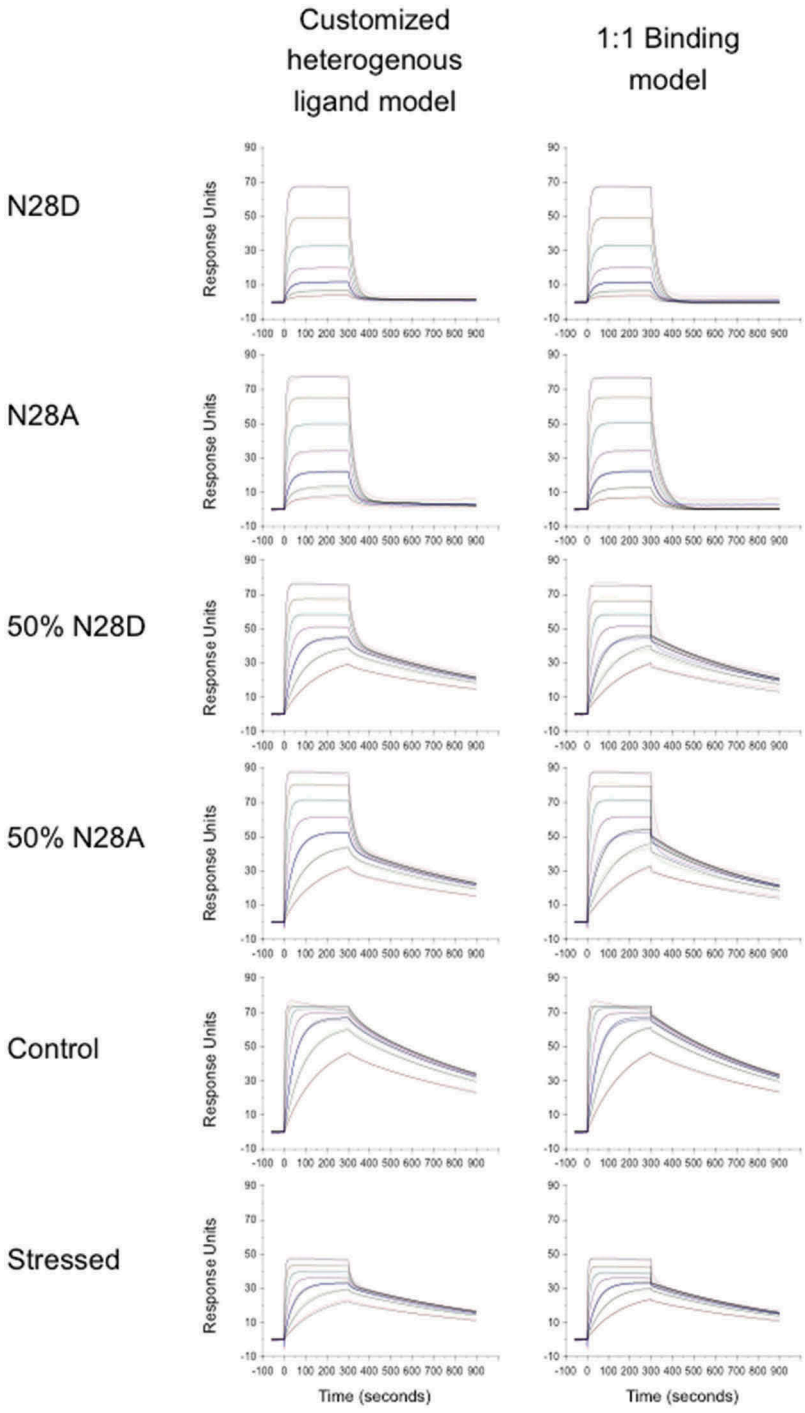

Figure 3. Similar antigen-binding SPR profiles are observed for the stressed sample and a mixture of Antibody #1 with deamidation surrogate mutation N28D.

Kinetic evaluation of control and stressed Antibody #1 samples and variants. Analyte concentrations used were 6.25–400 nM. Fitting results are shown overlaid (black lines). Left panels: Data were fit to the heterogenous ligand model modified to set the following parameters as constants: ka1, 7.6×10^5; kd1, 1.1×10^{-3}; RI, 0. Right panels: The same binding data as shown on the left fit to the 1:1 binding model. Note that the lower magnitude of the observed binding signal for the stressed antibody compared to the N28D/N28 antibody mixture suggests that the stressed antibody contains an additional subset with lower affinity for the antigen than the N28D deamidation product; the most likely reason for this is presence of the iso-Asp deamidation product, which is expected to occur in approximately three-fold excess over the N28D deamidation product (Figure 1).

heterogenous ligand model returned a KD value for the second interaction that was in good agreement with the experimentally determined KD of the N28D antibody (Table 2). In addition, the nRmax returned for the mixture of Antibody#1 and N28D mutant was 51% that of the nRmax for Antibody #1 alone, closely reflecting the theoretical proportion of Antibody #1 in the mixture (Table 2). Similar results were obtained with an alternative affinity-reduced variant of Antibody #1, an N28A mutant (Table 2).

The nRmax values obtained with the 1:1 binding model also approached the theoretical proportion of Antibody #1 in the mixed antibody samples; 55% of the reference nRmax for

Table 2. SPR analysis of the N28D mutant of Antibody #1, alone and as a mixture with Antibody #1.

			Heterogenous Ligand Model								1:1 Binding Model				
Isotype	Variable regions	Ligand Level (RU)	Chi² (RU²)	KD1 (nM)	KD2 (nM)	Rmax1 (RU)	Rmax2 (RU)	nRmax1	nRmax2	nRmax1 (% Ref.)	Chi² (RU²)	KD (nM)	Rmax (RU)	nRmax	nRmax (% Ref.)
"Q"	Antibody #1	230.5	2.0	1.8	21	72.6	7.6	0.31	0.05	Mean = Ref.	1.0	1.8	76.2	0.33	Mean = Ref.
	Antibody #1	230.2	0.3	1.8	37	76.1	6.1	0.33	0.04		0.3	1.4	76.6	0.33	
	Antibody #1	231.4	0.3	1.8	46	75.1	6.4	0.32	0.05		0.3	1.5	75.8	0.33	
	Antibody #1	226.0	0.5	1.8	37	75.1	6.7	0.33	0.05		0.4	1.4	75.7	0.33	
	Antibody #1, N28D	254.6	0.6	1.8	247	2.2	105.0	0.01	0.69	3%	1.6	160	81.0	0.32	96%
	Antibody #1, 50% N28D	252.5	0.4	1.8	199	41.7	51.5	0.17	0.34	51%	3.7	2.0	46.4	0.18	55%
	Antibody #1, N28A	251.0	1.4	1.8	108	5.2	91.7	0.02	0.61	6%	6.8	61	68.1	0.27	82%
	Antibody #1, 50% N28A	271.0	0.6	1.8	94	43.9	53.8	0.16	0.33	50%	5.2	2.1	50.9	0.19	57%
"P"	Antibody #1, Control	214.0	0.6	1.8	23	66.1	8.2	0.31	0.06	95%	0.6	1.5	68.8	0.32	97%
	Antibody #1, Stressed	217.3	0.4	1.8	150	32.2	20.0	0.15	0.15	46%	0.4	1.5	33.4	0.15	46%

the Antibody #1/N28D mixture and 57% for the Antibody #1/N28A mixture (Table 2). The reason for this result becomes apparent upon visual inspection of the sensorgrams and fitting data (Figure 3). In the examples shown, the interaction with the faster off-rate appears to be modeled by the Biacore parameter "RI", which is defined as "bulk refractive index contribution in the sample",[38] and is visible in the lower panels of Figure 3 as vertical lines at the beginning and end of the antigen injections. Because this low affinity and rapidly dissociating binding is attributed by the model to "bulk refractive index contribution", it is not included in the output value for Rmax. In this case, where the higher and lower affinities differ widely, the Rmax values reflect predominantly the higher affinity antibody population that is present.

The results also demonstrated that a mixture of the parental antibody and the N28D deamidation surrogate had a similar SPR profile to that observed with the stressed parental antibody, and, when fit with either the modified heterogenous ligand model or the 1:1 binding model, a corresponding decrease in nRmax. We concluded that this assay could be used to evaluate additional antibody samples for stress-induced changes that affect target binding, including cases where the affinity is not eliminated but is substantially reduced in comparison to the starting material.

HTP screening of diverse mutations for improved stability

In an attempt to stabilize the antibody against deamidation induced by thermal stress, we generated a panel of engineered variants and evaluated them using the SPR method described above. Variants (Supplementary Table 1) were designed using approaches that included reversion to mouse germline sequences, rational design and near-saturation mutagenesis of position 28. Due to the close proximity of another asparagine residue at light chain position 30 (VL.N30), position 30 was also extensively mutagenized (Supplementary Table 1). A panel of variants in which G29 was replaced by alanine (Supplementary Table 1) was also evaluated. Some variants were excluded from the study following unfavorable binding results in earlier experiments (data not shown). Ninety antibody variants were expressed at 1 ml scale, purified,[39] and then stressed by incubation at 40°C in phosphate-buffered saline (PBS) for two weeks. Stressed and unstressed samples were analyzed by SPR and changes in the binding capacity following thermal stress were evaluated by dividing the nRmax of the stressed sample by the nRmax of the unstressed sample. We will refer to the results of this calculation as the relative activity of the stressed antibody. For simplicity and to keep the number of fitting variables low, we calculated nRmax using the 1:1 binding model. Results for the affinities and the relative activities of the stressed antibodies are shown in Figure 4A and are also listed in Supplementary Table 1.

Values calculated for KD and relative activity both varied widely and are not obviously correlated. Variants with improved affinity were not detected (Figure 4A). In contrast, values for the relative activity ranged from below 30% to 100%, compared to 73% for Antibody #1 (Figure 4A, Supplementary Table 1). The results also confirmed the difficulty of N28 replacement, with all 16 mutants analyzed in either a D1 or E1 context showing at least a four-fold loss in affinity (Figure 4B). Mutation of the light chain residue 1 from Glu to Asp did not appear to affect affinity (Figure 4B, LC residue 28 = N, K, L, R).

Only one antibody (#54) demonstrated both a minimally impacted KD and a high relative activity (Figure 4A). The increased relative activity was surprising because the single F33L mutation responsible (compare antibody #2 with antibody #54, Table 3) was five residues downstream of N28, although still located within CDR-L1. The mutation was generated as part of a series of mutants investigating reversion of selected antibody residues back to the murine antibody germline sequence (D2V, L4M, F33L and L93H). These mutations were analyzed individually and in combination. For each of these mutations, results were therefore available for seven pairs of antibodies that differed only by that mutation (Table 3). We analyzed the effects of the mutation in each of the seven pairs (Figure 5). The mutation L93H had a consistently negative effect on both affinity and stability (Figure 5). The mutations L4M and F33L reduced (L4M) or increased (F33L) the relative activity in 6/7 and 5/7 cases, respectively (Figure 5B). The impact of F33L and L4M mutation was particularly notable in the case of Antibody #2,

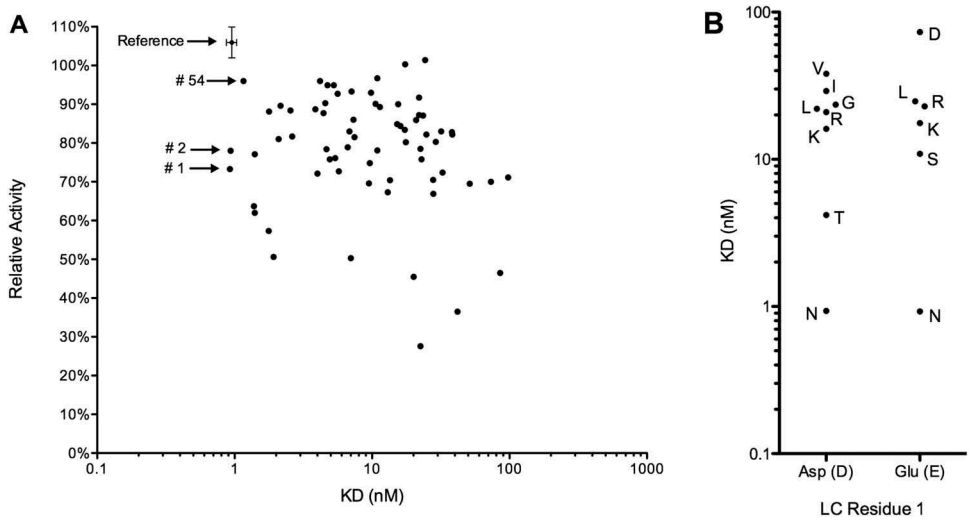

Figure 4. Impact of light chain mutations on affinity for target (KD) and resistance to thermal stress-induced specific activity loss.

A: Relative activity plotted against unstressed KD. Datapoints that did not meet initial QC criteria of Chi2 < 10% Rmax or nRmax (pre-stress) > 0.1 are not shown in this figure. Unstressed reference antibody data were obtained at the beginning, middle and end of each run (mean and standard deviation of nine datapoints in total). Datapoints for antibodies #1, #2 and #54 are labelled with the antibody number. B: Affinity data for N28X mutants. Datapoints are labelled with the identity of amino acid X in single letter code and separated according to the identity of the residue at position 1. Eight additional variants with X = F, H, P, Y, A, E, H, Q did not meet initial QC criteria (see above) and are not shown. X = M, W or C were not tested.

Table 3. Sequences of combinatorial germline reversion mutations D2V, L4M, F33L and L93H (adapted from Supplementary Table 1 and subject to initial QC criteria as described for Figure 4).

Variant	VL residues at selected locations (Kabat numbering)									KD (nM)	Relative Activity
Unstressed control (mean, n = 9)	**E**	**D**	**L**	**N**	**G**	**N**	**T**	**F**	**L**	**1.0**	**106%**
Antibody_01	E	D	L	N	G	N	T	F	L	0.9	73%
Antibody_02	D	D	L	N	G	N	T	F	L	0.9	78%
Antibody_51	D	V	L	N	G	N	T	F	L	3.9	89%
Antibody_52	D	D	M	N	G	N	T	F	L	1.8	57%
Antibody_53	D	V	M	N	G	N	T	F	L	4.7	95%
Antibody_54	D	D	L	N	G	N	T	L	L	1.2	96%
Antibody_55	D	V	L	N	G	N	T	L	L	7.1	93%
Antibody_56	D	D	M	N	G	N	T	L	L	1.8	88%
Antibody_57	D	V	M	N	G	N	T	L	L	11.4	89%
Antibody_58	D	D	L	N	G	N	T	F	H	32.6	72%
Antibody_59	D	V	L	N	G	N	T	F	H	17.3	83%
Antibody_60	D	D	M	N	G	N	T	F	H	41.8	37%
Antibody_61	D	V	M	N	G	N	T	F	H	22.5	78%
Antibody_62	D	D	L	N	G	N	T	L	H	38.3	82%
Antibody_63	D	V	L	N	G	N	T	L	H	27.8	70%
Antibody_64	D	D	M	N	G	N	T	L	H	51.4	70%

where F33L or L4M mutation resulted in the relative activity value changing from 78% to 96% and 57%, respectively (Table 3). Interestingly, we also noticed cooperativity between positions 2 and 93. The D2V mutation had a negative effect on affinity if residue 93 was leucine, but a positive effect on affinity if residue 93 was histidine (Figure 5A), and the negative effect of L93H on the antibody KD appeared lessened when position 2 was mutated to valine (Figure 5A, Table 3).

Validation of deamidation-resistance mutations identified by HTP screening

In order to validate whether improvements in the relative activity observed in the HTP assay were indicative of improved resistance to deamidation, antibodies #25, #26, #35, #56 and #54 (Table 4) were selected for scaled-up production followed by thermal stress and evaluation of stressed and unstressed material using MS. The selected antibodies, which gave relative activity values from 75% to 96% and represent variants with mutations in light chain residues 29, 30 and 33, were re-expressed, purified and stressed at pH 5.5 and pH 7.4. Deamidation levels at residues N28 and, where present, N30 were quantitated by LC-MS. The results indicated a correlation between the relative activity values obtained by the screen and the sum of the stress-induced deamidation on N28 and N30 in PBS at pH 7.4 as quantitated by LC-MS (R^2 = 0.97, Figure 6A). The correlation observed for this set of parameters was much tighter than that observed for N28 alone (Figure 6B). This is consistent with the negative impact of both N28D and N30D mutations on affinity (Supplementary Table 1).

The LC-MS results also confirmed that Antibody #54, containing the CDR-L1 mutation F33L, was resistant to light chain deamidation at both N28 and N30 (Table 4). This result was further confirmed by the observation of deamidation resistance for Antibody #54 formatted as a different isotype (Table 4). We also transferred the CDR-L1 mutation F33L onto a humanization variant of Antibody #1. This variant, Antibody #91, comprises the same heavy chain variable region as Antibody #1; however, the light chain was humanized onto a Kappa 1 backbone, in comparison to Kappa 2 backbone used for Antibody #1. The F33L mutation also improved the stability of light chain residue N28 in Antibody #91, while maintaining N30 stability (Table 4).

Discussion

The SPR assay we describe here uses an antibody capture format and focuses specifically on the ratio of the antibody-target response level to the antibody immobilization level,

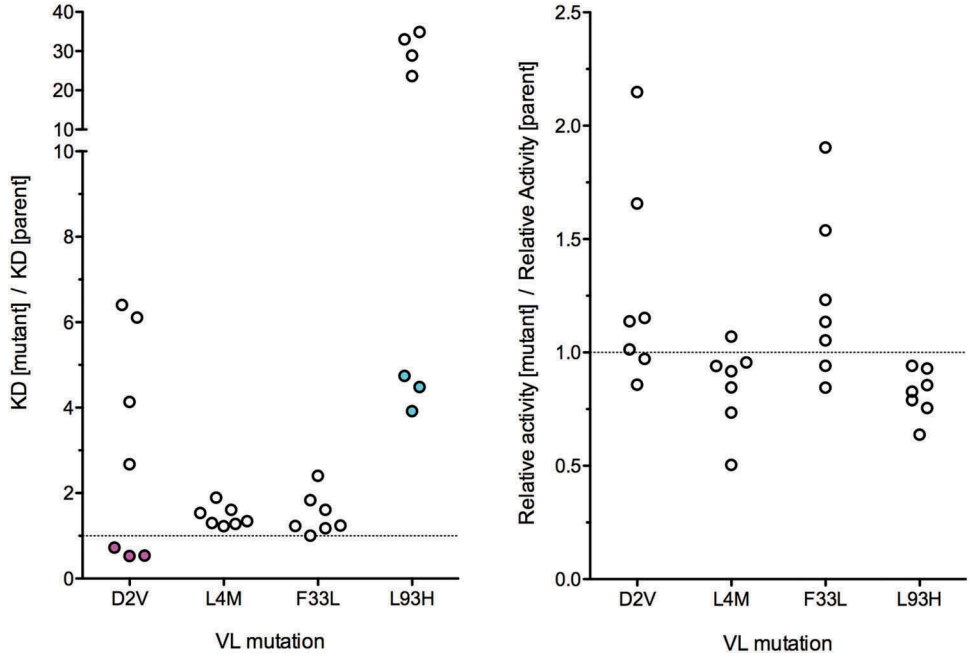

Figure 5. Impact of light chain mutations D2V, L4M, F33L and L93H on affinity for target (KD) and resistance to thermal stress-induced relative activity loss.
All data shown is from the fourteen variants detailed in Table 3 in which both variants met the initial QC criteria described in Figure 4 and which differ from each other at VL positions 2, 4, 33 and 93 only. Fold difference in KD (A) and relative activity (B) were calculated for matched antibody pairs within this set (a matched pair is defined here as two antibodies with sequences that differ only by the mutation indicated on the x axis). Figure 5A, far left column: mauve indicates presence of L93H mutation. Figure 5A, far right column: turquoise indicates presence of D2V mutation.

Table 4. Increase in N28 and N30 deamidation after two week stress test, determined by LC-MS.

			40C, pH 5.5		37C, pH 7.4	
Variant	N28 motif	Isotype	N28	N30	N28	N30
Antibody #1	NGNT	Q	11.1	Not detected	Not tested	Not tested
Antibody #25	NDNT	Q	9.1	24.1	17.4	24.0
Antibody #26	NTNT	Q	7.5	11.4	8.8	17.6
Antibody #35	NGQT	Q	11.9	N/A	17.9	N/A
Antibody #56 (F33L, L4M)	NGNT	Q	3.5	No increase detected	14.9	No increase detected
Antibody #54 (F33L)	NGNT	Q	2.8	0.2	5.3	No increase detected
		R	No increase detected	No increase detected	10.4	1.9
Antibody #91	NGNT	Q	15.7	0.4	Not tested	Not tested
Antibody #91 + F33L	NGNT	R	2.7	No increase detected	17.9	No increase detected

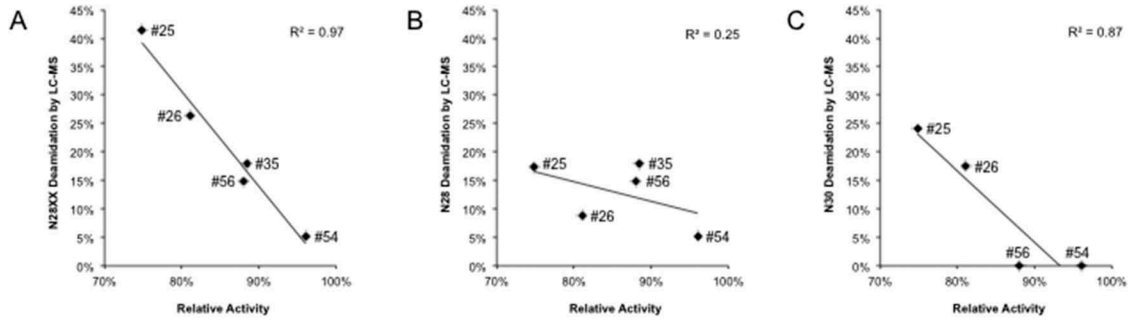

Figure 6. Correlation of relative activity determined by HTP screen with larger-scale stress-induced N28 or N28 + N30 deamidation determined by LC-MS.
Data shown are from Supplementary Table 1 and Table 4. Datapoints represent antibodies #25, #26, #35, #56 and #54. The y-axis shows the sum of stress-induced deamidation on (A) CDR-L1 N28 and, where present, N30; (B) on CDR-L1 N28 alone; (C) on CDR-L1 N30 alone.

similarly to that mentioned by Jarasch and colleagues.[8] Antibody capture formats can reduce interference by avidity effects and typically avoid requirements for time-consuming optimization of target-specific regeneration conditions. In contrast to calibration-based assays, the method used here focuses on antigen binding at or near saturation. Under sub-saturating conditions, binding response in an antibody capture assay is expected to depend on the interaction affinity, the analyte concentration, the specific activity of the captured antibody population; and under non-equilibrium conditions,

it will also depend on binding kinetics. At saturation however, the analyte binding response should depend solely on the specific activity. Focusing on saturation enables useful results to be obtained with a single reference sample in place of a standard curve.

In this report, we analyzed a heterogeneous population of modified and un-modified antibodies using a HTP antigen-binding kinetics experiment performed in an antibody capture format, and the resulting Rmax values were analyzed in relation to the amount of antibody captured. We used this method in combination with microplate-based accelerated thermal stress testing to screen 90 antibody variants for affinity and resistance to affinity-impacting asparagine deamidation. The results illustrate that the effect of a given mutation on the affinity for antigen can be decoupled from the effect of the mutation on the resistance of the antibody to thermal stress. In our hands, some mutations appear to affect affinity but not stability, others affect stability with minimal impact on affinity, and some seem to affect both affinity and stability (Figure 4). In addition, we found that the sum of stress-induced deamidation of VL.N28 and VL.N30 correlated more closely with relative activity than did deamidation of VL.N28 alone (Figure 6). This illustrates the advantage of assays based on target binding for screening purposes, by reducing the risk of advancing a mutation that fixes one problem but inadvertently causes another.

The results of this screen enabled rapid identification of a mutation in the + 5 position as an unexpectedly stabilizing influence on an otherwise deamidation-prone CDR-L1 asparagine residue. The F33L mutation conferred stability to this asparagine within two different VL frameworks and on two different isotypes. The mechanism by which the F33L mutation stabilizes N28 is not clear. We think it is unlikely that the F33L mutation compensates for deamidation via affinity improvement for several reasons: 1) the improvement in N28 deamidation resistance to thermal stress was validated by MS (Table 4); 2) similar KD values were obtained for unstressed 33L and 33F antibodies (compare antibodies #2 and #54, Table 3); and 3) the calculation method used here to determine relative activity is based on the parameter Rmax, which is an indicator of binding capacity and is therefore expected to be largely orthogonal to affinity. This latter point contrasts with methods based on comparison to reference curves at sub-saturating concentrations, and is an advantage of the Rmax-based method that we used in this study. Crystal structures of two antibodies with light chains similar to Antibody #1 indicate that the F33 residue may not be in direct contact with residues 28–31, but located in the light chain core (Figure 7). Therefore, residue 33, and perhaps residue 4 against which it packs within the core, may indirectly affect N28 stability of Antibody #1 by modulating conformational stability of the light chain.

In summary, we show here that changes in specific activity of an antibody sample can be detected in a fast, simple SPR-based assay and used as a surrogate metric to screen for resistance to chemical modification by accelerated thermal stress test. Application of this assay to an antibody susceptible to deamidation at a specific CDR asparagine side chain

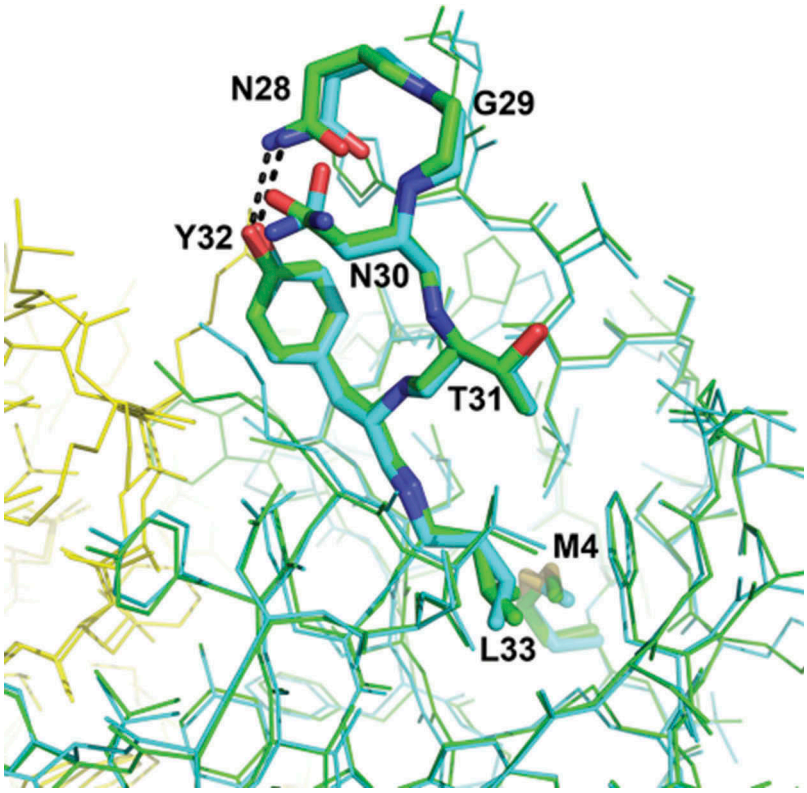

Figure 7. Structure of two unrelated antibodies with light chains similar to Antibody-A, PDB 4LEX, humanized (green) and PDB 1A4J, murine (cyan).
The heavy chains of both molecules are shown in yellow. Light chain residues 4 and 28 to 33 are indicated for both molecules. Residues 4 and 33 are Met and Leu respectively in both molecules.

enabled identification of an unexpected stabilizing mutation, which was transferable to an alternately humanized variant. Importantly, the improved resistance to deamidation induced by thermal stress was confirmed by LC-MS-based deamidation analysis.

This work focuses on asparagine deamidation following thermal stress, but it is likely that the methods described could also be applicable to other chemical modifications, including but not limited to methionine and tryptophan oxidation and isomerization of aspartyl residues. It may also facilitate evaluation of the impact of extrinsic conditions on chemical stability (Supplementary Figure 4). It is important to note that modifications that do not affect affinity will not be detected by this assay, and that if the affinity of the modified antibody for antigen is relatively similar to that of the parental antibody, the presence of these modifications may difficult or impossible to detect using this method. Ideally, the antigen should be monodisperse and monovalent, in order to minimize deviations from a 1:1 binding model that are not due to induced modifications. To confidently distinguish reductions in relative activity that are due to chemical modification from those reductions that are due to physical effects such as aggregation, confirmation studies (for example by LC-MS) are strongly recommended. However, the binding assay described uses laboratory equipment routinely available in antibody discovery and engineering laboratories and can provide stability data less than three weeks following the availability of microgram quantities of protein. Thus, this method represents a useful screen for rapid identification of stable variants, particularly at the earlier stages of therapeutic antibody research, and is an excellent complement to more direct but lower-throughput bioanalytical analyses.

Materials and methods

Protein production

For screening, antibodies were expressed as described previously.[39] For evaluation of stress-induced deamidation by MS, recombinant antibodies were produced by transient transfection of CHO cells with recombinant DNA and purified by affinity chromatography. Unless stated otherwise, residue numbering follows the Kabat system. Antigen protein for SPR was also expressed recombinantly and the monomeric status of the purified protein was confirmed by size exclusion chromatography with multi-angle static light scattering .

Surface plasmon resonance analysis

SPR experiments were performed using a Biacore T200 instrument (GE Life Sciences, Pittsburgh, PA, USA) with an analysis temperature of 25°C and Hepes-buffered saline running buffer (10 mM HEPES pH 7.4, 150 mM sodium chloride, 0.05% Tween 20). Human IgG capture chips were generated by amine coupling using the human IgG capture kit (GE Life Sciences, product code BR100839) and Series S CM5 chips (GE Life Sciences, product code BR100530). In this format, a human IgG (hIgG) capture reagent is covalently immobilized on the SPR chip surface, generating a hIgG-binding surface that is readily regenerated between cycles. Each cycle, samples containing hIgG were immobilized non-covalently by injection over the surface, followed by an injection of the analyte. Data were analyzed using Biacore Evaluation Software (GE Life Sciences). Unless stated otherwise, data were fit to a 1:1 binding model using default parameters, which include local fitting of the Biacore parameter RI. The equilibrium dissociation constant (KD) was calculated from the resulting association rate constant (ka) and dissociation rate constant (kd) and unless stated otherwise is reported from evaluation of the unstressed samples. Normalized Rmax (nRmax) was calculated by dividing the output value Rmax by the capture level ("Ligand Level"). Relative activity was calculated by dividing the nRmax of the stressed sample by the nRmax of the unstressed sample. The N28D mutant of Antibody #1 was analyzed by SPR, both alone and as a 1:1 mixture with the parental N28 antibody using the heterogenous ligand and the 1:1 binding models of the Biacore Evaluation Software. The values for ka1 and kd1 in the heterogenous ligand model were set as the average values of the ka and kd of four Antibody #1 samples analyzed using the 1:1 Binding Model to 7.6×10^5 $M^{-1}s^{-1}$ (ka1) and 1.1×10^{-3} s^{-1} (kd1) with RI set to 0, thus fixing the value of KD1 at 1.8 nM. Normalized Rmax (nRmax) was calculated by dividing Rmax (RU) by the capture level (RU). Delta (**Δ**) values were calculated as follows: (value for control sample – value for stressed sample)/value for control sample.

Thermal stress

To produce "stressed" and "unstressed" samples for comparison in initial assays, a solution of 1 mg/ml Antibody #1 (isotype "P") was incubated at 40°C for two weeks at pH 7.4 in PBS, 100 mM sucrose. For analytical thermal stress measurements, antibody samples were incubated at 1 mg/ml in 20 mM histidine acetate, 240 mM sucrose, pH 5.5 for two weeks at 40°C or PBS, pH 7.4 for two weeks at 37°C. A control sample was stored at −70°C.

Microplate-format thermal stress test

Antibodies were expressed in microplate format by transient transfection of Expi293 cells followed by purification with MabSelect SuRe resin (GE Healthcare).[39] Briefly, antibodies were eluted into 160 µl 50 mM phosphoric acid pH 3 and neutralized with 12 µl 20x PBS pH 11, then diluted with PBS to a concentration of 0.1 mg/ml using a Hamilton Star liquid handler (Hamilton Robotics, Reno, NV, USA). 100 µl samples were transferred to a 96-well microplate (VWR North America, catalog no. 83007–372) that was sealed with Microseal® 'B' PCR plate sealing film (BioRad, catalog no. MSB1001). The samples were then stressed by incubation at 40°C in a GeneAmp™ PCR System 9700 instrument (Thermo Fisher Scientific, Waltham, MA, USA) for two weeks. The heated lid was used to avoid condensation of fluid on the plate seal and any consequent reduction in homogeneity of the local protein, salt or buffer concentration. Evaporative loss, calculated by comparing the weight of the sealed plate before and after the incubation, was 0.84 grams, less than 9% (w/v) of the liquid content. Kinetic analysis by SPR was performed on the stressed and unstressed proteins, using multi-cycle kinetics and analyte concentrations

of 0, 26.5 nM and 265 nM. Association and dissociation injections were 180 seconds and 300 seconds, respectively, with a flow rate of 40 µl/min.

Deamidation analysis by peptide mapping

Samples were reduced with 20 mM dithiothreitol in 6 M guanidine hydrochloride, 360 mM Tris, and 2 mM ethylenediaminetetraacetic acid at pH 8.6 for 1 hour. The reduced samples were cooled to room temperature and alkylated using 1 M iodoacetic acid (final concentration, 50 mM) for 15 minutes in the dark. The samples were then buffer-exchanged into digestion buffer (25 mM Tris, 2 mM $CaCl_2$, pH 8.2). The buffer-exchanged samples were digested with trypsin for 4 hours at 37°C using a 1:40 (w/w) enzyme to substrate ratio. The digestion was stopped by addition of formic acid to a final concentration of 3.0%.

Tryptic digests were analyzed using LC-MS on a Q Exactive™ Hybrid Quadrupole-Orbitrap™ instrument (Thermo Fisher Scientific). The system was interfaced with an Acquity UPLC® H-Class Bio system (Waters Corporation, Milford, MA, USA). Separations were carried out on a 1.7 µm, 130 Å, 2.1 x 150 mm, Acquity UPLC® CSH column (Waters Corporation) at a flow rate of 0.2 mL/min (45 min gradient), with mobile phases containing 0.1% formic acid in water (solvent A) and 0.1% formic acid in acetonitrile (solvent B). The column temperature was set to 77°C and a peptide mixture corresponding to 10 µg of protein was injected onto the column. Full scan accurate mass data was acquired at a resolution of 17,500 in positive ion mode scanning from 200 to 2000 *m/z*. Data was processed using Xcalibur™ software (Thermo Fisher Scientific).

Relative percent deamidation values were calculated by taking the peak areas of the extracted ion chromatograms for the deamidated peptide(s), dividing by the sum of the peak areas of extracted ion chromatograms the native and deamidated peptides, and multiplying by 100 (Supplementary Figures 2, 3). Deamidation values for stressed material were then compared to control samples to determine the increase in deamidation following stress. MS and MS/MS analysis allowed for localization of deamidation site to N28 and/or N30 (Supplementary Figures 2, 3). Length of the tryptic peptide containing light chain residue N28 was 31 residues for Antibody #1 and 23 residues for Antibody #91.

Abbreviations

3D: Three-dimensional
Asp: Aspartic acid
CDR: Complementarity-determining region
CHO: Chinese Hamster Ovary
hIgG: Human immunoglobulin G
HPLC: High pressure liquid chromatography
HTP: High throughput
Iso-Asp: Iso-aspartic acid
ka: Association rate constant
kd: Dissociation rate constant
KD: Equilibrium dissociation constant
LC: Liquid chromatography
Leu: Leucine
M: Molar
Met: Methionine
mM: Millimolar
MS: Mass spectrometry
nM: Nanomolar
nRmax: Normalized Rmax
PBS: Phosphate-buffered saline
PCR: Polymerase chain reaction
PIMT: Protein L-isoaspartyl methyltransferase
QC: Quality control
SPR: Surface plasmon resonance
VL: Antibody light chain variable region
w/v: Weight/volume
w/w: Weight/weight
µl: Microliters
µl/min: Microliters per minute

Acknowledgments

We would like to acknowledge Peter Luan (Genentech) for high throughput protein purifications, Yongmei Chen (Genentech) for assistance in obtaining antibody variant DNA constructs and Jason Schumer (GE Life Sciences) and John Quinn (Genentech) for helpful discussions.

Disclosure of interest

All authors are or were employees of Genentech, a member of the Roche group, and may hold stock or other financial interests in F. Hoffmann-La Roche Ltd. Genentech has a commercial interest in therapeutic antibody products and antibody engineering technologies.

References

1. Miller PC, Xu P. Considerations in mRelative Activityanufacturing process development for antibody-based therapeutics. In: Tabrizi MA, Bornstein GG, Klakamp SL, editors.Development of antibody-based therapeutics: translational considerations. New York (NY): Springer New York; 2012. p. 355–373.
2. Liu H, Gaza-Bulseco G, Faldu D, Chumsae C, Sun J. Heterogeneity of monoclonal antibodies. J Pharm Sci. 2008;97:2426–2447. doi:10.1002/jps.21180.
3. Manning MC, Chou DK, Murphy BM, Payne RW, Katayama DS. Stability of protein pharmaceuticals: an update. Pharm Res. 2010;27:544–575.
4. Shire SJ. Formulation and manufacturability of biologics. Curr Opin Biotechnol. 2009;20:708–714. doi:10.1016/j.copbio.2009.10.006.
5. Wang W, Singh S, Zeng DL, King K, Nema S. Antibody structure, instability, and formulation. J Pharm Sci. 2007;96:1–26. doi:10.1002/jps.20727.
6. Daugherty AL, Mrsny RJ. Formulation and delivery issues for monoclonal antibody therapeutics. Adv Drug Deliv Rev. 2006;58:686–706. doi:10.1016/j.addr.2006.03.011.
7. Volkin DB, Hershenson S, Ho RJY, Uchiyama S, Winter G, Carpenter JF. Two decades of publishing excellence in pharmaceutical biotechnology. J Pharm Sci. 2015;104:290–300. doi:10.1002/jps.24285.
8. Jarasch A, Koll H, Regula JT, Bader M, Papadimitriou A, Kettenberger H. Developability assessment during the selection of novel therapeutic antibodies. J Pharm Sci. 2015;104:1885–1898. doi:10.1002/jps.24430.
9. Yang X, Xu W, Dukleska S, Benchaar S, Mengisen S, Antochshuk V, Cheung J, Mann L, Babadjanova Z, Rowand J, et al.. Developability studies before initiation of process development: improving manufacturability of monoclonal antibodies. mAbs. 2014;283:16194–16205.
10. Geiger T, Clarke S. Deamidation, isomerization, and racemization at asparaginyl and aspartyl residues in peptides. Succinimide-linked reactions that contribute to protein degradation. J Biol Chem. 1987;262:785–794.

11. Riggs DL, Gomez SV, Julian RR. Sequence and solution effects on the prevalence of d-isomers produced by deamidation. ACS Chem Biol. 2017;12:2875–2882. doi:10.1021/acschembio.7b00686.
12. Wright HT, Urry DW. Nonenzymatic deamidation of asparaginyl and glutaminyl residues in proteins. Crit Rev Biochem Mol Biol. 1991;26:1–52. doi:10.3109/10409239109081719.
13. McKerrow JH, Robinson AB. Primary sequence dependence of the deamidation of rabbit muscle aldolase. Science. 1974;183:85. doi:10.1126/science.183.4120.85.
14. Robinson AB, Rudd CJ. Deamidation of glutaminyl and asparaginyl residues in peptides and proteins. Curr Top Cell Regul. 1974;8:247–295.
15. Robinson NE, Robinson ZW, Robinson BR, Robinson AL, Robinson JA, Robinson ML, Robinson AB. Structure-dependent nonenzymatic deamidation of glutaminyl and asparaginyl pentapeptides. J Pept Res. 2004;63:426–436. doi:10.1111/jpp.2004.63.issue-5.
16. McKerrow JH, Robinson AB. Deamidation of asparaginyl residues as a hazard in experimental protein and peptide procedures. Anal Biochem. 1971;42:565–568. doi:10.1016/0003-2697(71)90074-1.
17. Kossiakoff AA. Tertiary structure is a principal determinant to protein deamidation. Science. 1988;240:191–194. doi:10.1126/science.3353715.
18. Robinson NE, Robinson AB. Prediction of protein deamidation rates from primary and three-dimensional structure. Proc Natl Acad Sci U S A. 2001;98:4367–4372. doi:10.1073/pnas.071066498.
19. Sydow JF, Lipsmeier F, Larraillet V, Hilger M, Mautz B, Mølhøj M, Kuentzer J, Klostermann S, Schoch J, Voelger HR, et al.. Structure-based prediction of asparagine and aspartate degradation sites in antibody variable regions. PLoS One. 2014;9:e100736. doi:10.1371/journal.pone.0100736.
20. Jia L, Sun Y. Protein asparagine deamidation prediction based on structures with machine learning methods. PLoS One. 2017;12:e0181347. doi:10.1371/journal.pone.0181347.
21. Parr MK, Montacir O, Montacir H. Physicochemical characterization of biopharmaceuticals. J Pharm Biomed Anal. 2016;130:366–389. doi:10.1016/j.jpba.2016.05.028.
22. Robinson AB, McKerrow JH, Cary P. Controlled deamidation of peptides and proteins: an experimental hazard and a possible biological timer. Proc Natl Acad Sci U S A. 1970;66:753–757.
23. Hao P, Ss A, Gallart-Palau X, Sk S. Recent advances in mass spectrometric analysis of protein deamidation. Mass Spectrom Rev. 2016;9999:1–16.
24. Tran JC, Tran D, Hilderbrand A, Andersen N, Huang T, Reif K, Hötzel I, Stefanich EG, Liu Y, Wang J. Automated affinity capture and on-tip digestion to accurately quantitate in vivo deamidation of therapeutic antibodies. Anal Chem. 2016;88:11521–11526. doi:10.1021/acs.analchem.6b02766.
25. Reubsaet JL, Beijnen JH, Bult A, Van Maanen RJ, Marchal JA, Underberg WJ. Analytical techniques used to study the degradation of proteins and peptides: chemical instability. J Pharm Biomed Anal. 1998;17:955–978. doi:10.1016/S0731-7085(98)00063-6.
26. Harris RJ. Heterogeneity of recombinant antibodies: linking structure to function. Dev Biol (Basel). 2005;122:117–127.
27. Aswad DW, Paranandi MV, Schurter BT. Isoaspartate in peptides and proteins: formation, significance, and analysis. J Pharm Biomed Anal. 2000;21:1129–1136. doi:10.1016/S0731-7085(99)00230-7.
28. Lowenson JD, Clarke S. Recognition of D-aspartyl residues in polypeptides by the erythrocyte L-isoaspartyl/D-aspartyl protein methyltransferase. Implications for the repair hypothesis. J Biol Chem. 1992;267:5985–5995.
29. Hsiao K, Alves J, Patel R, Adams M, Nashine V, Goueli S. A high-throughput bioluminescent assay to monitor the deamidation of asparagine and isomerization of aspartate residues in therapeutic proteins and antibodies. J Pharm Sci. 2017;106:1528–1537. doi:10.1016/j.xphs.2017.02.022.
30. Athmer L, Kindrachuk J, Georges F, Napper S. The influence of protein structure on the products emerging from succinimide hydrolysis. J Biol Chem. 2002;277:30502–30507. doi:10.1074/jbc.M205314200.
31. Vlasak J, Bussat MC, Wang S, Wagner-Rousset E, Schaefer M, Klinguer-Hamour C, Kirchmeier M, Corvaïa N, Ionescu R, Beck A. Identification and characterization of asparagine deamidation in the light chain CDR1 of a humanized IgG1 antibody. Anal Biochem. 2009;392:145–154. doi:10.1016/j.ab.2009.05.039.
32. Gandhi S, Ren D, Xiao G, Bondarenko P, Sloey C, Ricci MS, Krishnan S. Elucidation of degradants in acidic peak of cation exchange chromatography in an IgG1 monoclonal antibody formed on long-term storage in a liquid formulation. Pharm Res. 2012;29:209–224. doi:10.1007/s11095-012-0843-0.
33. Haberger M, Bomans K, Diepold K, Hook M, Gassner J, Schlothauer T, Zwick A, Spick C, Kepert JF, Hienz B, et al.. Assessment of chemical modifications of sites in the CDRs of recombinant antibodies: susceptibility vs. functionality of critical quality attributes. mAbs. 2014;6:327–339. doi:10.4161/mabs.27876.
34. Haberger M, Heidenreich A-K, Schlothauer T, Hook M, Gassner J, Bomans K, Yegres M, Zwick A, Zimmermann B, Wegele H, et al.. Functional assessment of antibody oxidation by native mass spectrometry. mAbs. 2015;7:891–900. doi:10.1080/19420862.2015.1052199.
35. Gassner C, Lipsmeier F, Metzger P, Beck H, Schnueriger A, Regula JT, Moelleken J. Development and validation of a novel SPR-based assay principle for bispecific molecules. J Pharm Biomed Anal. 2015;102:144–149. doi:10.1016/j.jpba.2014.09.007.
36. Meschendoerfer W, Gassner C, Lipsmeier F, Regula JT, Moelleken J. SPR-based assays enable the full functional analysis of bispecific molecules.J Pharm Biomed Anal. 2017;132:141–147. doi:10.1016/j.jpba.2016.10.009.
37. GE Healthcare Life Sciences. Human Antibody Capture Kit, Instruction 22-0648-88 AD, 22nd ed. Pittsburgh (PA): GE Healthcare Bio-Sciences; 2007.
38. GE Life Sciences. BiacoreTM T200 software handbook, 28th ed. Pittsburgh (PA): GE Healthcare Bio-Sciences; 2010.
39. Bos AB, Luan P, Duque JN, Reilly D, Harms PD, Wong AW. Optimization and automation of an end-to-end high throughput microscale transient protein production process. Biotechnol Bioeng. 2015;112:1832–1842. doi:10.1002/bit.25601.